Origin of multiferroicity in $MnWO_4$

I. V. Solovyev*

Computational Materials Science Unit, National Institute for Materials Science, 1-2-1 Sengen, Tsukuba, Ibaraki 305-0047, Japan

(Received 29 October 2012; revised manuscript received 25 March 2013; published 4 April 2013)

$MnWO_4$ is regarded as a canonical example of multiferroic materials, where the multiferroic activity is caused by a spin-spiral alignment. We argue that, in reality, $MnWO_4$ has two sources of the spin spirality, which conflict with each other. One source is the Dzyaloshinskii-Moriya (DM) interactions, reflecting the $P2/c$ symmetry of the lattice. The $P2/c$ structure of $MnWO_4$ has an inversion center that connects two Mn sublattices. Therefore, from the viewpoint of DM interactions, different Mn sublattices are expected to have *opposite* spin chirality. Another source is competing isotropic exchange interactions, which tend to form a spin-spiral texture with *the same* chirality in both magnetic sublattices. Thus there is a conflict between DM and isotropic exchange interactions, which makes these two sublattices inequivalent and, therefore, breaks the inversion symmetry. Our theoretical analysis is based on the low-energy model, derived from first-principles electronic structure calculations.

DOI: 10.1103/PhysRevB.87.144403 PACS number(s): 75.30.−m, 75.85.+t, 71.15.Rf, 73.22.Gk

I. INTRODUCTION

The idea of breaking the inversion symmetry by some complex magnetic order has attracted a great deal of attention. It gives rise to the phenomenon of improper ferroelectricity, where the ferroelectric (FE) polarization is induced by the magnetic order and, therefore, can be controlled by the magnetic field. Alternatively, one can change the magnetic structure by applying the electric field. This makes multiferroic materials promising for the creation of the new generation of electronic devices.[1,2]

One of magnetic textures that breaks the inversion symmetry is the spin spiral. Moreover, this property is universal, in a sense that it can take place in all types of magnetic compounds, irrespectively of their symmetry, as long as the the spin-spiral order is established.[3] Probably, this is the reason why the idea of the spin-spiral alignment became so popular in the field of multiferroics: many properties of such compounds are interpreted from the viewpoint of spin-spiral order,[4–6] and the search for new multiferroic materials is frequently conducted around those with the spin-spiral order.[2]

Nevertheless, the spin-spiral alignment alone is insufficient for having a FE activity: although the spin-spiral order breaks the inversion symmetry, one can always find some appropriate uniform rotation of spins, which transforms the inverted spin spiral to the original one (see Appendix). The FE polarization in such a situation will be equal to zero. In order to make it finite (and in order to fully break the inversion symmetry), one should ban the possibility of uniform rotations in the system of spins. This can be done by the relativistic spin-orbit (SO) interaction, and today it is commonly accepted in the theory of multiferroic materials that the spin-spiral alignment should be always supplemented with the SO coupling.[4,6] However, as long as the SO coupling is involved, the spin-spiral texture becomes deformed. Then, we face the question whether the FE activity is caused by the spin-spiral order itself or by the deviation from it.[7] The answer to this question is very important for understanding the origin of multiferroicity.

$MnWO_4$ is an important material in the field of multiferroics. Although the transition temperature to the multiferroic phase is low and the FE polarization is weak, the material is fundamentally important, because (i) its multiferroic phase has a spin-spiral texture (or it is believed to be the spin spiral) and (ii) the relative directions of the spin-spiral propagation vector, the spin rotation axis, and the FE polarization seem to be consistent with predictions based on the spin-spiral theory.[8–10] Thus $MnWO_4$ is regarded as one of successful manifestations of the spin-spiral theory and, actually, the discovery of the FE activity in $MnWO_4$ was guided by this theory.

More specifically, $MnWO_4$ crystallizes in the monoclinic $P2/c$ structure. It exhibits three successive antiferromagnetic (AFM) transitions: at $T_{N3} \sim 13.5$ K, $T_{N2} \sim 12.5$ K, and $T_{N1} \sim 7.6$ K. The AF1 phase, realized below T_{N1}, is nearly collinear and the directions of spins alternate along the monoclinic $\boldsymbol{a}$ axis as $\uparrow\uparrow\downarrow\downarrow$ (the reason why the AF1 phase is sometimes called the "$\uparrow\uparrow\downarrow\downarrow$ phase"). The incommensurate AF2 phase, realized in the temperature interval $T_{N1} < T < T_{N2}$, is typically ascribed to the spin spiral with the propagation vector $\mathbf{q}_{AF2} = (-0.214, 1/2, 0.457)$ (in units of reciprocal lattice translations). The AF3 phase ($T_{N2} < T < T_{N3}$) is characterized by a collinear sinusoidally modulated AFM order with the same $\mathbf{q} = \mathbf{q}_{AF2}$. The AF2 phase is ferroelectric. The polarization vector is parallel to the monoclinic $\boldsymbol{b}$ axis: $\mathbf{P} = (0, P_b, 0)$. P_b is relatively small: it takes a maximal value (~ 50 μC/m^2) at around T_{N1}, then monotonously decreases and vanishes at around T_{N2}.[8] Other phases display no sign of FE activity.

In this work, we will argue that the multiferroicity in $MnWO_4$ has a more complex origin. Namely, we will show that, in order to obtain finite polarization, (i) it is not sufficient to have a simple homogeneous spin-spiral texture and (ii) the spin spiral should be deformed by some conflicting interactions, existing in the system. In $MnWO_4$, these are Dzyaloshinskii-Moriya (DM) interactions and isotropic exchange interactions. The conflict of these two interactions breaks the inversion symmetry and gives rise to the FE activity in the AF2 phase.

II. METHOD

We follow the same strategy as in our previous publications, devoted to multiferroic manganites.[7] Our basic idea is to construct a realistic low-energy (Hubbard-type) model for the Mn $3d$ bands, which would describe basic magnetic

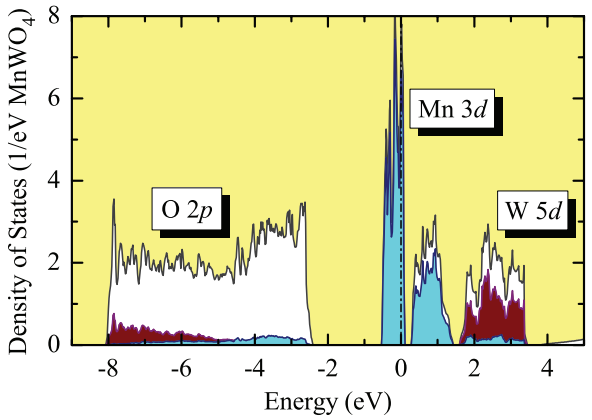

FIG. 1. (Color online) Total and partial densities of states of $MnWO_4$ in the local density approximation. The shaded light (blue) and dark (brown) areas show the contributions of the Mn $3d$ and W $5d$ states, respectively. The positions of the main bands are indicated by symbols. The Fermi level is at zero energy (shown by dot-dashed line).

properties of $MnWO_4$ at a semiquantitative level. The model is constructed in the basis of Wannier orbitals, starting from electronic structure calculations in the local density approximation (LDA) with and without the relativistic SO interaction. The Mn $3d$ bands split into the lower-lying t_{2g} and upper-lying e_g subbands, located at around -0.2 and 0.8 eV, respectively (see Fig. 1). All these bands are well separated from the rest of the spectrum. In this case, the Wannier basis is complete and the construction of the model Hamiltonian is rather straightforward. More specifically, the Wannier functions were constructed by the projector-operator method, using atomic Mn $3d$ orbitals as the trial functions. Thus the main weight of the Wannier functions is located at the Mn sites, and small tails spread to the O and W sites. In the Wannier basis, the one-electron part of the model Hamiltonian exactly reproduces the original LDA band structure. The parameters of screened Coulomb and exchange interactions in the Mn $3d$ band were computed by using the combined approach, incorporating the constrained LDA and the random-phase approximation for the screening. Other details can be found in the review article (see Ref. 11). All calculations have been performed using experimental parameters of the crystal structure.[12] Since heavy W atoms are an important source of relativistic interactions, the SO coupling was included at the level of ordinary LDA calculations, and thus the obtained electronic structure was used as the starting point for the construction of the low-energy model. Thus, although the W sites were not explicitly included to the model, the relativistic effects, associated with these sites, were allowed to contribute to the dispersion of the Mn $3d$ bands and, therefore, were taken into account in the low-energy model. All parameters of the model Hamiltonian are collected in Ref. 13. After the construction, the model was solved in the mean-field Hartee-Fock (HF) approximation.

We would also like to briefly comment on merits and demerits of our technique in comparison with the ordinary first-principles approach.

(i) It is certainly true that the construction of the model Hamiltonian is based on some additional approximations,[11] and is sometimes regarded as a step back in comparison with ordinary first-principles calculations. On the other hand, it would not be right to think that the first-principles calculations for the transition-metal oxides are free of any approximations. The necessity to treat the problem of on-site Coulomb correlations, which is frequently formulated in terms of the LDA + U approach (with some phenomenological correction "+U", borrowed from the Hubbard model) make it similar to the model approach: it also relies on additional approximations, although of a different type. The typical approximations are the choice of the parameter U and the form of the double-counting term, which are both ill-defined in the LDA + U.[14] Thus, at the present stage, it would not be right to say that one techniques is more superior than other; rather, they provide a complementary information for the analysis of material properties of the transition-metal oxides. As we will see below, results of our model analysis are well consistent with available first-principles calculations for $MnWO_4$.[15,16]

(ii) The search of the ground state for noncollinear magnetic textures can be very time consuming, even at the level of mean-field HF approximation: the rotations of magnetic moments towards new equilibrium directions after including the SO interaction can be very slow and require tens of thousands of iterations, as in the case of $MnWO_4$. In such a situation, the model Hamiltonian approach is very useful, because it allows us to find a fully self-consistent magnetic texture, which is not always accessible for the ordinary first-principles calculations.[7]

(iii) The model Hamiltonian approach can be very useful for the analysis and interpretation of results of complex electronic structure calculations and the experimental data. Particularly, in this work, it will help us to elucidate the microscopic origin of the magnetic inversion symmetry breaking in $MnWO_4$. We will also show that the experimental behavior of long-range magnetic interactions in $MnWO_4$ (see Ref. 17) can be naturally understood in the framework of the superexchange (SE) theory and reflects similar behavior of the transfer integrals in the low-energy model.

III. RESULTS AND DISCUSSIONS

First, we solve the low-energy model in the HF approximation, by assuming the collinear ferromagnetic (FM) alignment of spins, and derive parameters of isotropic exchange interactions. For these purposes we employ the theory of infinitesimal spin rotations.[11,18] The procedure corresponds to the local mapping of the change of the one-electron energy onto isotropic spin Hamiltonian of the Heisenberg form $\mathcal{H}_{\rm H} = -\sum_{i>j} J_{ij}\mathbf{e}_i \cdot \mathbf{e}_j$, where $\mathbf{e}_i$ is the *direction* of spin at the site i and the summation run over *inequivalent pairs* of sites. The results of these calculations are explained in Fig. 2. Alternatively, one can apply the theory of superexchange (SE) interactions, by considering the energy gain caused by virtual hoppings ($t_{ij}^{mm'}$) in the second order of perturbation theory.[19] For the d^5 configuration of Mn^{2+}, this expression is extremely simple: $J_{ij} = -\sum_{mm'} t_{ij}^{mm'} t_{ji}^{m'm}/\Delta_{\rm ex}$, where $\Delta_{\rm ex}$ is the intraatomic splitting between the majority- and minority-spin states and the summation runs over all $3d$ orbitals: m (m') = xy, yz, $3z^2 - r^2$, zx, and $x^2 - y^2$.[20] Thus all SE interactions are expected to be antiferromagnetic. Then, by

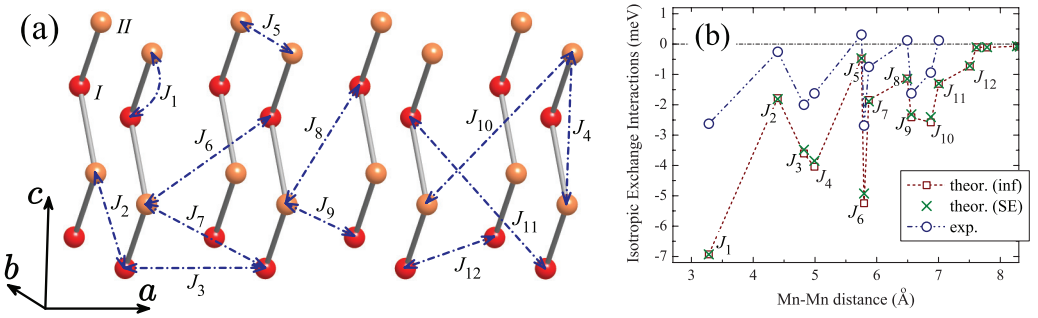

FIG. 2. (Color online) (a) Lattice of Mn sites with the notations of isotropic exchange interactions (numbered in the increasing order of interatomic distances). Note that the $P2/c$ structure of $MnWO_4$ has two Mn sublattices, which are shown by different colors and denoted as "I" and "II", respectively. These sublattices are transformed to each other by the inversion operation. (b) Distance dependence of isotropic exchange interactions: results of calculations, using the theory of infinitesimal spin rotations near the ferromagnetic state (denoted as "inf") and the theory of superexchange interactions with $\Delta_{ex} = 5$ eV (denoted as "SE"), in comparison with the experimental data from Ref. 17.

taking $\Delta_{ex} = 5$ eV and using the values of $t_{ij}^{mm'}$, which were obtained for the low-energy model (see Ref. 13), one can find that the SE theory excellently reproduces results of the more general theory of infinitesimal spin rotations. Moreover, in the framework of the Hubbard model, Δ_{ex} can be estimated as $\Delta_{ex} \approx U + 4J_H$. The values of averaged on-site Coulomb repulsion U and the intraatomic exchange interaction J_H, derived for the low-energy model, are 1.8 and 0.8 eV, respectively.[13] This yields $\Delta_{ex} = 5$ eV. Thus all estimates are consistent with each other. Therefore one may conclude that (i) the physically relevant mechanism, responsible for isotropic exchange interactions in $MnWO_4$, is the superexchange, and (ii) the experimental distance-dependence of J_{ij} reflects similar behavior of the transfer integrals $t_{ij}^{mm'}$.

Our calculations capture main details of the experimental distance-dependence of J_{ij} (see Fig. 2).[17] This is a very important finding, which means that in our model we should be able to reproduce the correct magnetic structures of $MnWO_4$. The negative aspect is that our parameters J_{ij} are "too antiferromagnetic" (AFM). For example, the Curie-Weiss temperature can be estimated as $\theta_{CW} \approx \sum_j J_{ij}/3k_B$. Then, the obtained parameters J_{ij} yield $\theta_{CW} = -265$ K, which exceeds the experimental value -78 K (see Ref. 8) by factor three. The discrepancy cannot be resolved simply by changing the value of the on-site Coulomb repulsion U, which is frequently treated as an adjustable parameter. Particularly, in order to explain the existence of FM interactions, which were observed experimentally in some of the bonds,[17] we need an additional mechanism on the top of our model. Such a mechanism can be related to the magnetic polarization of the oxygen band, similar to orthorhombic manganites.[21] The first-principles GGA + U calculations (where GGA stands for the generalized gradient approximation—an extension of LDA) also substantially overestimate $|J_{ij}|$ and $|\theta_{CW}|$.[15] Although these calculations take into account the effect of the oxygen band, the disagreement is probably caused by additional approximations for the double-counting energy, which is ill-defined in GGA + U.[14] Finally, the experimental parameters J_{ij} themselves may be sensitive to the details of fitting of the spin-wave dispersion. In this respect, we would like to mention that earlier experimental data were interpreted in terms of rather different set of parameters J_{ij}.[22] Thus, at the present stage, taking into account the complexity of the problem of interatomic magnetic interactions in $MnWO_4$, the agreement between theoretical and experimental data in Fig. 2 can be regarded as satisfactory.

Then, we search the magnetic ground state of $MnWO_4$ without relativistic SO coupling. For these purposes, we employ the spin-spiral formalism, which is based on generalized Bloch theorem.[3] The idea is to combine the lattice translations with rotations in the spin subspace. It allows us to treat the incommensurate magnetic textures with an arbitrary vector $\mathbf{q} = (q_a, 1/2, q_c)$ such as if the magnetic unit contained only one crystallographic cell.[3] The results of these calculations, which were also performed in the HF approximation for the low-energy model, are summarized in Fig. 3. For $\mathbf{q} = (-1/4, 1/2, 1/2)$, the collinear $\uparrow\uparrow\downarrow\downarrow$ and noncollinear spin-spiral states are nearly degenerate. Nevertheless, the total energy of the spin spiral continues to decrease with the increase of q_a, and $MnWO_4$ is expected to form the spin-spiral ground state with $\mathbf{q}_{NR} \approx (-0.18, 1/2, 0.45)$, which is lower in energy than the $\uparrow\uparrow\downarrow\downarrow$ state by about 0.5 meV/Mn. Moreover, none of these states is ferroelectric: although the spin spiral breaks the inversion symmetry, the latter can be combined with an appropriate rotation of spins, which transforms the inverted

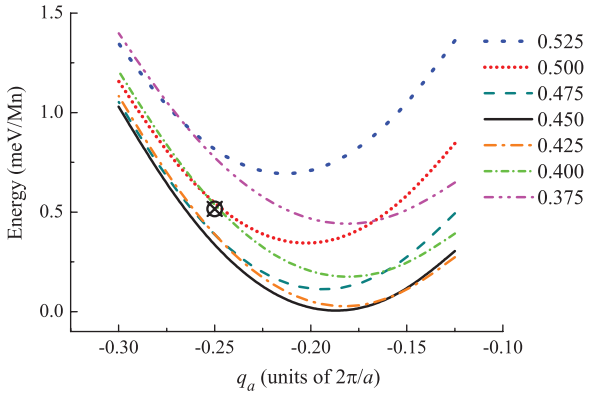

FIG. 3. (Color online) Results of Hartree-Fock calculations for the spin-spiral states with $\mathbf{q} = (q_a, 1/2, q_c)$: total energies versus q_a for different values of q_c (in units of $2\pi/c$). The energy of the collinear $\uparrow\uparrow\downarrow\downarrow$ state is marked by the symbol $\otimes$.

spin spiral to the original one (see Appendix). Thus the FE polarization will vanish.

Therefore we should find the answer to the following questions: (i) which interaction stabilizes the AF1 texture and make it the ground state of $MnWO_4$ at low T? (ii) What is the mechanism of the inversion-symmetry breaking in the AF2 phase, which yields finite P_b? For these purposes, we consider the relativistic SO interaction. It gives rise to such important ingredients as the single-ion anisotropy and DM interactions.

The effect of single-ion anisotropy on the magnetic texture of $MnWO_4$ can be studied by enforcing the atomic limit and setting all transfer integrals equal to zero.[23] Generally, the single-ion anisotropy is expected to be small for the nearly spherical d^5 configuration of Mn^{2+}. Since the symmetry operation $\{C_b^2|\boldsymbol{c}/2\}$ of the space group $P2/c$ transforms each Mn site to itself (here, C_b^2 stands for the 180° rotation around the $\boldsymbol{b}$ axis and $\boldsymbol{c}/2$ is the additional translation), the single-ion anisotropy will tend to align the spins either parallel to the $\boldsymbol{b}$ axis ($||\boldsymbol{b}$) or in the $\boldsymbol{ac}$ plane ($\in\boldsymbol{ac}$). In the latter case, the spins are canted off the $\boldsymbol{a}$ axis by about 41°, which is close to the experimental value of 35°.[8] The easy magnetization direction corresponds to the in-plane configuration. However, the energy difference between hard ($||\boldsymbol{b}$) and easy ($\in\boldsymbol{ac}$) magnetization directions is small (less that 0.05 meV/Mn), so that in the spin-spiral texture, it can be easily overcome by the energy gain caused by isotropic exchange interactions.

For discussing the DM interactions, it is more convenient to use the extended notations and recall that each site of the lattice i can be specified by its position $\boldsymbol{\tau}$ in the primitive cell and the translation $\boldsymbol{R}$. Then, since the $P2/c$ structure of $MnWO_4$ has two Mn-sublattices (denoted as "I" and "II" in Fig. 2), which can be transformed to each other by the inversion operation, the DM interactions will obey the following symmetry rules.[24] (i) All interactions between different sublattices are equal to zero. (ii) The DM interactions in each magnetic sublattice will depend only on the vector $\boldsymbol{R}$, connecting two Mn sites. Then, the DM interactions in the sublattices "I" and "II" will be related by the following identity $\mathbf{d}_{\boldsymbol{R}}^{I} = \mathbf{d}_{-\boldsymbol{R}}^{II} = -\mathbf{d}_{\boldsymbol{R}}^{II}$, which holds any $\boldsymbol{R}$ (note that $\mathbf{d}$ is the axial antisymmetric vector). Moreover, due to the symmetry operation $\{C_b^2|\boldsymbol{c}/2\}$, all DM vectors lie in the $\boldsymbol{ac}$ plane, i.e., similar to the easy magnetization direction, obtained from the analysis of the single-ion anisotropy.

To be specific, let us define the DM spin Hamiltonian as $\mathcal{H}_{\rm DM}^{I(II)} = \sum_{\boldsymbol{R}'>\boldsymbol{R}} \mathbf{d}_{\boldsymbol{R}'-\boldsymbol{R}}^{I(II)}[\mathbf{e}_{\boldsymbol{R}\pm\boldsymbol{\tau}} \times \mathbf{e}_{\boldsymbol{R}'\pm\boldsymbol{\tau}}]$, which is constructed separately for each magnetic sublattice. In these notations, $\mathbf{e}_{\boldsymbol{R}\pm\boldsymbol{\tau}}$ is the *direction* of spin, where $+\boldsymbol{\tau}$ and $-\boldsymbol{\tau}$ correspond to the sublattices I and II, respectively. Moreover, in each magnetic sublattice, we can shift the origin and place it in $+\boldsymbol{\tau}$ and $-\boldsymbol{\tau}$, respectively. Then, the DE spin Hamiltonian becomes $\mathcal{H}_{\rm DM}^{I(II)} = \sum_{\boldsymbol{R}'>\boldsymbol{R}} \mathbf{d}_{\boldsymbol{R}'-\boldsymbol{R}}^{I(II)}[\mathbf{e}_{\boldsymbol{R}} \times \mathbf{e}_{\boldsymbol{R}'}]$. Moreover, we use the convention where the sites $\boldsymbol{R}$ and $\boldsymbol{R}'$ order in the positive direction of the $\boldsymbol{a}$ axis, and $(\boldsymbol{R}' - \boldsymbol{R}) \cdot \boldsymbol{a} > 0$.

The parameters of DM interactions can be evaluated by considering the mixed type of perturbation theory expansion with respect to the SO coupling and infinitesimal rotations of spins near the FM state.[25] Then, the obtained changes of the one-electron energy can be mapped onto the DM Hamiltonian. It yields the following parameters of DM interactions (in meV): $\mathbf{d}_{\boldsymbol{a}}^{I} = (-0.01,0,0.01)$, $\mathbf{d}_{\boldsymbol{c}}^{I} = (-0.02,0,0.02)$, and $\mathbf{d}_{\boldsymbol{a}+\boldsymbol{c}}^{I} = (0.01,0,-0.01)$. Interactions in other bonds are considerably weaker.

The equilibrium magnetic texture, obtained after switching on the relativistic SO interaction in the collinear ↑↑↓↓ state, is explained in Fig. 4. Due to the single-ion anisotropy, all spins are confined mainly in the $\boldsymbol{ac}$ plane and canted off the $\boldsymbol{a}$ axis by about 46° (that is close to 41°, obtained in the atomic limit). The DM interactions yield an additional canting of spins out of the $\boldsymbol{ac}$ plane. The corresponding force $\mathbf{f}_{\boldsymbol{R}} = -\partial\mathcal{H}_{\rm DM}/\partial\mathbf{e}_{\boldsymbol{R}}$, experienced by the Mn spin at the site $\boldsymbol{R}$ from its neighboring sites in the same sublattice, is given by $\mathbf{f}_{\boldsymbol{R}} = \sum_{\boldsymbol{R}'}[\mathbf{d}_{\boldsymbol{R}'-\boldsymbol{R}} \times \mathbf{e}_{\boldsymbol{R}'}] \equiv \sum_{\boldsymbol{R}'}[\mathbf{d}_{\boldsymbol{R}'} \times \mathbf{e}_{\boldsymbol{R}+\boldsymbol{R}'}]$. Here, we drop the sublattice indices, because all the arguments equally apply to both magnetic sublattices. Since $\mathbf{d}_{-\boldsymbol{R}'} = -\mathbf{d}_{\boldsymbol{R}'}$, in order to contribute to $\mathbf{f}_{\boldsymbol{R}}$, the directions of neighboring spins should satisfy the following condition: $\mathbf{e}_{\boldsymbol{R}-\boldsymbol{R}'} = -\mathbf{e}_{\boldsymbol{R}+\boldsymbol{R}'}$. In the ↑↑↓↓ texture, such a situation takes place for $\boldsymbol{R}' = \boldsymbol{a}$ and $\boldsymbol{a}+\boldsymbol{c}$, but not for $\boldsymbol{R}' = \boldsymbol{c}$. Moreover, since both $\mathbf{d}$ and $\mathbf{e}$ lie in the $\boldsymbol{ac}$ plane, the force will be parallel to the $\boldsymbol{b}$ axis. Finally, due to the alternation of $\mathbf{e}$ in the ↑↑↓↓ texture, the directions of forces will also alternate. All in all, this explains fine details of the magnetic structure in Fig. 4(b). Very importantly, the isotropic exchange interactions, single-ion anisotropy, and DM interactions in the AF1 phase do not conflict with each other in a sense that all of them, even jointly, continue to respect the crystallographic $P2/c$ symmetry. Therefore the inversion symmetry is preserved and the polarization is equal to zero, even after including the SO interaction.[26]

The effect of SO interaction on the spins-spiral alignment can be best understood for $\mathbf{q} = (-1/4,1/2,1/2)$ (see Fig. 5). In this structure, the easy magnetization direction ($\mathbf{e} \in \boldsymbol{ac}$) at certain Mn-site alternates with the hard magnetization direction ($\mathbf{e}||\boldsymbol{b}$) at its neighboring sites. Thus there is a conflict between isotropic exchange interactions and the

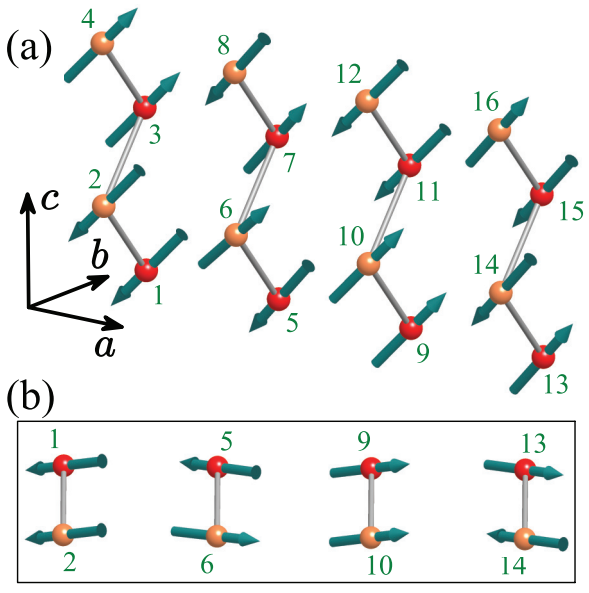

FIG. 4. (Color online) (a) Arrangement of spins in the AF1 phase, as obtained in the mean-field HF calculations for the low-energy model with relativistic SO interaction and (b) projection of spins onto the $\boldsymbol{ab}$ plane.

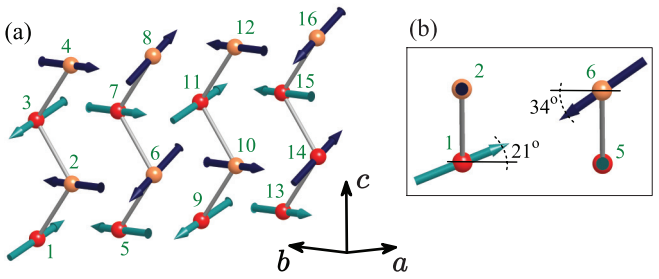

FIG. 5. (Color online) (a) The deformed spin-spiral texture with $\mathbf{q} = (-1/4, 1/2, 1/2)$, as obtained in the mean-field HF calculations for the low-energy model with the relativistic SO interaction, and (b) its projection onto the $\boldsymbol{ac}$ plane.

single-ion anisotropy. However, since the latter is small, this magnetic structure can be realized at a low-energy cost. Then, due to the DM interactions, each site with $\mathbf{e}||\boldsymbol{b}$ will experience a force from its neighboring sites with $\mathbf{e} \in \boldsymbol{ac}$. Since $\mathbf{d} \in \boldsymbol{ac}$, this force will be parallel to the $\boldsymbol{b}$ axis. Alternatively, each site with $\mathbf{e} \in \boldsymbol{ac}$ will experience the force from its neighboring sites with $\mathbf{e}||\boldsymbol{b}$. Since $\mathbf{d} \in \boldsymbol{ac}$, this force will also lie in the $\boldsymbol{ac}$ plane and additionally rotate the spin in this plane.

Furthermore, since $\mathbf{d}^{I}_{R'} = -\mathbf{d}^{II}_{R'}$, the forces in different sublattices will act *in the opposite directions*. The effect of these forces can be best understood in terms of the vector spin chirality. For a spin spiral, propagating along the $\boldsymbol{a}$ axis, all cross products $[\mathbf{e}_R \times \mathbf{e}_{R'}]$, constructed between the nearest neighbors, are the same, and such state can be described by the vector spin chirality $\boldsymbol{k} = [\mathbf{e}_R \times \mathbf{e}_{R'}]$. Obviously, if one considers the DM Hamiltonian alone, which can be defined separately for each magnetic sublattice, the direction of $\boldsymbol{k}$ will be controlled by the parameters of DM interactions. Then, since $\mathbf{d}^{I}_{R} = -\mathbf{d}^{II}_{R}$, in order to minimize the energy of DM interactions, similar relation should hold for the spin chirality: $\boldsymbol{k}^{I} = -\boldsymbol{k}^{II}$. This means that the DM interactions will tend to form the state with *opposite chirality* in two magnetic sublattices. However, the spin-spiral texture that is formed by isotropic exchange interactions J_{ij} has *the same chirality* in both magnetic sublattices. Therefore we have a conflict between isotropic and DM interactions: if in one magnetic sublattice the effect of these two interactions is added, in the other magnetic sublattice, it will be subtracted. All these tendencies are clearly seen in the fine details of the magnetic texture, obtained in the HF calculations, where we start from the homogeneous spin-spiral state and switch on the SO interaction (see Fig. 5). First, the canting of spins, lying in the $\boldsymbol{ac}$ plane, appears to be different for the sublattices I and II: 21° and 34°, respectively, relative to the $\boldsymbol{a}$ axis. Second, as discussed above, the spins with $\mathbf{e}||\boldsymbol{b}$ will experience the force $\mathbf{f}$, which is also parallel to $\boldsymbol{b}$. However, since $\mathbf{d}^{I}_{R} = -\mathbf{d}^{II}_{R}$, the vectors $\mathbf{e}$ and $\mathbf{f}$ at the same site will be either parallel or antiparallel, depending on the magnetic sublattice. Thus the magnitude of local spin magnetic moment with $\mathbf{e}||\boldsymbol{b}$ will also depend on the magnetic sublattice. Of course, the difference of the magnetic moments is small (about 0.01%, according to our HF calculations). Nevertheless, it does take place and is just another manifestation of the conflict between isotropic and DM interactions.

Thus the conflict between isotropic and DM interactions in the AF2 phase makes the sublattices I and II inequivalent. Since in the $P2/c$ structure, these two sublattices are connected by the inversion operation, their inequivalency means that the inversion symmetry is broken and the actual symmetry of the AF2 phase is lower than $P2/c$. Furthermore, the homogeneous spin-spiral alignment itself is deformed by the DM interactions and, strictly speaking, the AF2 phase is *no longer the spin spiral*. The magnitude of this deformation can be seen in the inset of Fig. 5.

Then, we discuss the relative stability of different magnetic phases with the SO interaction. In this case, the generalized Bloch theorem is not applicable and the only possibility is to work with the supercell geometry.[3] Therefore we were able to consider only the solutions with $\mathbf{q} = (q_a, 1/2, 1/2)$ and the rational $q_a = -1/3$, $-1/4$, and $-1/5$. The results can be summarized as follows. Amongst the AF2 states, the one with $q_a = -1/5$ has the lowest energy. The state with $q_a = -1/4$ is higher in energy by about 0.2 meV/Mn. This behavior is similar to calculations without SO coupling (see Fig. 3). Then, the AF2 state with $q_a = -1/5$ appears to be nearly degenerate with the AF1 state (the energy difference is about 0.07 meV/Mn, but the AF2 state is still low in energy). Although these numerical values are probably on the verge of accuracy of our model analysis, this tendency clearly shows that the SO interaction additionally stabilizes AF1 state relative to the AF2 one. This seems to be reasonable: the conflict of DM and isotropic exchange interactions, acting in the opposite directions in one of the Mn sublattices, will penalize the energy of the AF2 state. On the other hand, in the AF1 state, there is no such conflict and the DM interactions will additionally minimize the energy of the $\uparrow\uparrow\downarrow\downarrow$ texture, obtained without SO interaction. Apparently, the main reason why the energy of the AF2 phase is still slightly lower than that of the AF1 phase is related to the fact that the isotropic exchange interactions are overestimated in our low-energy model (see Fig. 2) and, therefore, the effect of the SO coupling and DM interactions on the magnetic texture is underestimated.

Finally, we evaluate the value of the FE polarization in the AF2 phase, using the Berry phase formalism,[27] which was adopted for the low-energy model.[7] Here, we calculate only the electronic contribution, which arises in the centrosymmetric $P2/c$ structure due to the magnetic inversion symmetry breaking. However, we do not consider the structural relaxation in response to this magnetic symmetry breaking. The vector of polarization is parallel to the $\boldsymbol{b}$ axis, in agreement with the experiment.[8] Then, the value of P_b can be estimated as 2.0, 3.8, and 4.4 $\mu C/m^2$ for $q_a = -1/3$, $-1/4$, and $-1/5$, respectively. Thus P_b is small, but it is well consistent with the fact that the DM interactions are also small and lead only to small perturbation of the homogeneous spin-spiral texture, that is formed by the isotropic exchange interactions. Nevertheless, we would like to emphasize that the DM interactions are essential for deforming the spin spiral, breaking the inversion symmetry, and producing the finite value of P_b.

The experimental polarization is an order of magnitude larger: $P_b \sim 50$ $\mu C/m^2$.[8] However, it can be still regarded as a "small value" in comparison with many other multiferroic systems.[1] Therefore it is quite consistent with our main idea

that P_b is a result of a small perturbation of the spin-spiral texture, caused by the relativistic effects.

There may be several reasons why the experimental value of P_b is larger than the theoretical one. (i) The experimental P_b may also include some lattice effects, in response to lowering of the magnetic symmetry.[16] (ii) An unusual aspect of $MnWO_4$ is that the inversion symmetry is broken in the "high-temperature" phase, while the low-temperature phase remains centrosymmetric (for comparison, the situation in perovskite manganites is exactly the opposite).[1] Thus, in addition to the FE polarization, one should find some mechanism, which would explain the AF1→AF2 phase transition at finite T. This mechanism may involve some temperature effects. (iii) The low-energy model is designed for the semiquantitative analysis. It is not always possible to expect a good quantitative agreement with the experimental data, because some ingredients can be missing in the model. In principle, the GGA + U calculations are also of a semiquantitative level, because the value of P_b depends on the adjustable parameter U.[28] In our model analysis, the small value of P_b may be related to the overestimation of isotropic exchange interactions (see Fig. 2). Then, the deformation of the spin-spiral texture, caused by the relativistic effects, is underestimated. Therefore the value of P_b is also underestimated. From this point of view, the behavior of isotropic exchange interactions, the total energies, and the FE polarization is consistent with each other, and the main efforts towards quantitative description of the FE polarization and the phase diagram of $MnWO_4$ should be concentrated on the quantitative description of isotropic exchange interactions.

IV. SUMMARY

In summary, we have provided the microscopic explanation for the origin of FE activity in $MnWO_4$. The multiferroicity in this compound is caused by the conflict of DM and isotropic exchange interactions in the AF2 phase. Thus $MnWO_4$ is multiferroic not simply because of the spiral texture. It is essential to have conflicting interactions, which deform the spin spiral, break the inversion symmetry, and, thus, give rise to the FE activity.

Here, one can also make some analogy with the weak ferromagnetism.[24] In the AFM materials, two magnetic sublattices are connected by the time-reversal operation. The SO interaction can break this time-reversal symmetry and under certain conditions, related to the symmetry of the crystal and the type of the AFM order, give rise to the phenomenon of weak ferromagnetism. One of microscopic interactions, responsible for this effect, is the DM interaction. In the $P2/c$ structure of $MnWO_4$, two sublattices are connected by the spacial inversion. Thus the $MnWO_4$ can be regarded as an antiferroelectric material. The SO interactions can break the inversion symmetry and give rise to a weak FE polarization. Thus, in an analogy with the weak ferromagnetism, this phenomenon can be called "weak ferroelectricity." On the microscopic level, it is also related to the behavior of DM interactions. Again, like in weak ferromagnetism, the existence of the weak ferroelectricity in $MnWO_4$ depends on two factors: (i) the specific symmetry of the crystal (in our case, the $P2/c$ symmetry), and (ii) the specific type of the magnetic order (in our case, the AF2 order). It should not be confused with some general properties of the spin spiral.

ACKNOWLEDGMENT

This work is partly supported by the grant of the Ministry of Education and Science of Russia No. 14.A18.21.0889.

APPENDIX: NONEXISTENCE OF FERROELECTRICITY IN HOMOGENEOUS SPIN-SPIRAL STATE WITHOUT SPIN-ORBIT INTERACTION

In this Appendix, we will show that, although the spatial inversion is not the symmetry operation of the homogeneous spin-spiral state, it can be always combined with an appropriate rotation of spins, which transforms the inverted spin-spiral texture to the original one. The ferroelectric polarization in such a situation will be equal to zero. The prove is extremely simple, but first we would like to illustrate the basic idea on a cartoon picture for the one-dimensional spin spiral (see Fig. 6). The basic property of the spin spiral is such that: if $\mathbf{e}$ is the direction of spin at certain magnetic site and $\hat{\mathcal{I}}\mathbf{e}$ is the direction of spin at the same site after the inversion of the lattice, one can always define the axis $\mathbf{n}||(\mathbf{e}+\hat{\mathcal{I}}\mathbf{e})$, which has the same direction at all magnetic sites. Then, the inverted spin spiral can be transformed to the original one by the uniform 180° rotation of spins around this axis.

Now, we will provide a rigorous prove of this statement. To be specific, consider the situation, realized in $MnWO_4$ and assume that there are two sites in the primitive cell, which are located at $\boldsymbol{\tau}$ and $-\boldsymbol{\tau}$, respectively. Thus these two cites can be transformed to each other by the inversion operation $\hat{\mathcal{I}}$ and the inversion center is located in the origin. Then, the translations $\boldsymbol{R}$ will specify the location of all other inversion centers, while the atomic position will be given by the vectors $\boldsymbol{R}\pm\boldsymbol{\tau}$.

In the spin-spiral texture, the directions of magnetic moments are given by

$$\mathbf{e}_{\boldsymbol{R}\pm\boldsymbol{\tau}} = \begin{pmatrix} \cos \mathbf{q}\cdot(\boldsymbol{R}\pm\boldsymbol{\tau}) \\ \sin \mathbf{q}\cdot(\boldsymbol{R}\pm\boldsymbol{\tau}) \\ 0 \end{pmatrix}. \tag{A1}$$

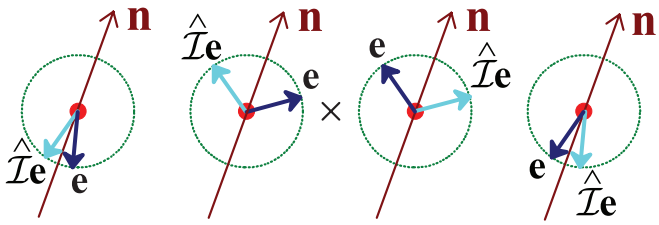

FIG. 6. (Color online) Cartoon picture, explaining how the inverted spin spiral can be transformed to the original one by the uniform rotation of spins. The inversion center is marked by cross. The directions of magnetic moments in the original spin spiral ($\mathbf{e}$) are shown by the dark (blue) vectors, and those in the inverted spin spiral ($\hat{\mathcal{I}}\mathbf{e}$) are shown by the light (cyan) vectors. The inverted spin-spiral texture can be transformed to the original one by the 180° rotation of spins around the axis $\mathbf{n}||(\mathbf{e}+\hat{\mathcal{I}}\mathbf{e})$, which has the same direction at all sites of the lattice.

For our purposes, it is sufficient to consider the situation where all spins rotate in the $\boldsymbol{ab}$ plane. The generalization for an arbitrary orientation of the rotation plane is straightforward and will be discussed at the end of this Appendix.

Consider the inversion around an arbitrary center $\boldsymbol{R}_0$. It transforms an arbitrarily taken site $\boldsymbol{R} \pm \boldsymbol{\tau}$ to $\boldsymbol{R}_0 - (\boldsymbol{R} \pm \boldsymbol{\tau} - \boldsymbol{R}_0) = 2\boldsymbol{R}_0 - \boldsymbol{R} \mp \boldsymbol{\tau}$. Then, the direction of spin at the site $2\boldsymbol{R}_0 - \boldsymbol{R} \mp \boldsymbol{\tau}$ will change from $\mathbf{e}_{2\boldsymbol{R}_0 - \boldsymbol{R} \mp \boldsymbol{\tau}}$ to $\mathbf{e}_{\boldsymbol{R} \pm \boldsymbol{\tau}}$. Thus our goal is to find a transformation $\hat{\mathcal{R}}$, which would rotate $\mathbf{e}_{\boldsymbol{R} \pm \boldsymbol{\tau}}$ back to $\mathbf{e}_{2\boldsymbol{R}_0 - \boldsymbol{R} \mp \boldsymbol{\tau}}$. This transformation is the 180° rotation around the axis $\mathbf{n} || (\mathbf{e}_{2\boldsymbol{R}_0 - \boldsymbol{R} \mp \boldsymbol{\tau}} + \mathbf{e}_{\boldsymbol{R} \pm \boldsymbol{\tau}})$. The corresponding rotation matrix is given by

$$\hat{\mathcal{R}} = \begin{pmatrix} \cos(2\mathbf{q} \cdot \boldsymbol{R}_0) & \sin(2\mathbf{q} \cdot \boldsymbol{R}_0) & 0 \\ \sin(2\mathbf{q} \cdot \boldsymbol{R}_0) & -\cos(2\mathbf{q} \cdot \boldsymbol{R}_0) & 0 \\ 0 & 0 & -1 \end{pmatrix}.$$

Indeed, using the expressions for $\mathbf{e}_{2\boldsymbol{R}_0 - \boldsymbol{R} \mp \boldsymbol{\tau}}$ and $\mathbf{e}_{\boldsymbol{R} \pm \boldsymbol{\tau}}$, given by Eq. (A1), it is straightforward to verify that $\hat{\mathcal{R}} \mathbf{e}_{\boldsymbol{R} \pm \boldsymbol{\tau}} = \mathbf{e}_{2\boldsymbol{R}_0 - \boldsymbol{R} \mp \boldsymbol{\tau}}$. Since $\hat{\mathcal{R}}$ does not depend on $\boldsymbol{R}$, it corresponds to the uniform rotation of spins. Without SO coupling, the spin system is fully isotropic and such transformation is permissible. Thus, although $\hat{\mathcal{I}}$ is formally broken, $\hat{\mathcal{R}}\hat{\mathcal{I}}$ is the symmetry operation, which transforms the spin spiral to itself. Since the uniform rotation of spins $\hat{\mathcal{R}}$ does not affect the polarization, the existence of the symmetry operation $\hat{\mathcal{R}}\hat{\mathcal{I}}$ means that the ferroelectric activity in the homogeneous spin-spiral state is forbidden.

This is a general property of the spin-spiral—although we have considered a specific lattice geometry, which is more relevant to $MnWO_4$, absolutely the same argument can be repeated, for example, for orthorhombic manganites, where the magnetic sites are located in the centers of inversion. The only requirement is that the lattice itself has inversion symmetry and for each site, $\boldsymbol{R} + \boldsymbol{\tau}$, its image, $\hat{\mathcal{I}}(\boldsymbol{R} + \boldsymbol{\tau})$, can be also found amongst the lattice sites.

For an arbitrary orientation of the spin rotation plane, $\mathbf{e}_{\boldsymbol{R} \pm \boldsymbol{\tau}}$ in Eq. (A1) should be replaced by $\hat{\mathcal{D}}\mathbf{e}_{\boldsymbol{R} \pm \boldsymbol{\tau}}$, where $\hat{\mathcal{D}}$ is the rotation of the $\boldsymbol{ab}$ plane. Then, all above arguments apply after replacing $\hat{\mathcal{R}}$ by $\hat{\mathcal{D}}\hat{\mathcal{R}}\hat{\mathcal{D}}^{-1}$.

*solovyev.igor@nims.go.jp

[1] Y. Tokura, Science **312**, 1481 (2006); S.-W. Cheong and M. Mostovoy, Nat. Mater. **6**, 13 (2007); D. Khomskii, Physics **2**, 20 (2009).

[2] T. Kimura, Annu. Rev. Mater. Res. **37**, 387 (2007); Y. Tokura and S. Seki, Adv. Mater. **22**, 1554 (2010).

[3] L. M. Sandratskii, Adv. Phys. **47**, 91 (1998).

[4] H. Katsura, N. Nagaosa, and A. V. Balatsky, Phys. Rev. Lett. **95**, 057205 (2005).

[5] M. Mostovoy, Phys. Rev. Lett. **96**, 067601 (2006).

[6] I. A. Sergienko and E. Dagotto, Phys. Rev. B **73**, 094434 (2006).

[7] I. V. Solovyev, Phys. Rev. B **83**, 054404 (2011); I. V. Solovyev, M. V. Valentyuk, and V. V. Mazurenko, *ibid.* **86**, 144406 (2012).

[8] K. Taniguchi, N. Abe, T. Takenobu, Y. Iwasa, and T. Arima, Phys. Rev. Lett. **97**, 097203 (2006).

[9] A. H. Arkenbout, T. T. M. Palstra, T. Siegrist, and T. Kimura, Phys. Rev. B **74**, 184431 (2006).

[10] O. Heyer, N. Hollmann, I. Klassen, S. Jodlauk, L. Bohatý, P. Becker, J. A. Mydosh, T. Lorenz, and D. Khomskii, J. Phys.: Condens. Matter **18**, L471 (2006).

[11] I. V. Solovyev, J. Phys.: Condens. Matter **20**, 293201 (2008).

[12] G. Lautenschläger, H. Weitzel, T. Vogt, R. Hock, A. Böhm, M. Bonnet, and H. Fuess, Phys. Rev. B **48**, 6087 (1993).

[13] See Supplemental Material at http://link.aps.org/supplemental/10.1103/PhysRevB.87.144403 for parameters of the crystal field, transfer integrals, and matrices of Coulomb interactions.

[14] I. V. Solovyev and K. Terakura, Phys. Rev. B **58**, 15496 (1998).

[15] C. Tian, C. Lee, H. Xiang, Y. Zhang, C. Payen, S. Jobic, and M.-H. Whangbo, Phys. Rev. B **80**, 104426 (2009).

[16] K. V. Shanavas, D. Choudhury, I. Dasgupta, S. M. Sharma, and D. D. Sarma, Phys. Rev. B **81**, 212406 (2010).

[17] F. Ye, R. S. Fishman, J. A. Fernandez-Baca, A. A. Podlesnyak, G. Ehlers, H. A. Mook, Y. Wang, B. Lorenz, and C. W. Chu, Phys. Rev. B **83**, 140401(R) (2011).

[18] A. I. Liechtenstein, M. I. Katsnelson, V. P. Antropov, and V. A. Gubanov, J. Magn. Magn. Matter. **67**, 65 (1987).

[19] P. W. Anderson, Phys. Rev. **115**, 2 (1959).

[20] Note that in the atomic limit, all majority-spin states are occupied and the minority-spin states are empty. Therefore, for the antiferromagnetically coupled spins, the virtual hoppings from the subspace of occupied states at the site i to the subspace of unoccupied states at the site j will involve all combinations of the orbital indices m and m'. Furthermore, the energy cost for transferring an electron between two atomic sites is Δ_{ex} (the energy splitting between occupied and empty states in the atomic limit). All together, this explains the expression for the superexchange interactions.

[21] I. Solovyev, J. Phys. Soc. Jpn. **78**, 054710 (2009).

[22] H. Ehrenberg, H. Weitzel, H. Fuess, and B. Hennion, J. Phys.: Condens. Matter **11**, 2649 (1999).

[23] I. V. Solovyev, Phys. Rev. B **85**, 054420 (2012).

[24] I. Dzyaloshinsky, J. Chem. Phys. Solids **4**, 241 (1958); T. Moriya, Phys. Rev. **120**, 91 (1960).

[25] I. Solovyev, N. Hamada, and K. Terakura, Phys. Rev. Lett. **76**, 4825 (1996).

[26] More specifically, the AF1 phase can be transformed to itself by combining the spacial inversion, the translation $\boldsymbol{R} = \pm\boldsymbol{a}$, and (optionally) the time-reversal operation (depending on the translation and the location of the inversion center).

[27] D. Vanderbilt and R. D. King-Smith, Phys. Rev. B **48**, 4442 (1993); R. Resta, J. Phys.: Condens. Matter **22**, 123201 (2010).

[28] Two groups reported reported rather different values of P_b, depending on the parameter U: $P_b \sim 17.2\ \mu\mathrm{C/m^2}$ (see Ref. 15, for $U = 6$ eV) and $P_b \sim 42\ \mu\mathrm{C/m^2}$ (see Ref. 16, for $U = 4$ eV).